Resistance-change devices based on solid electrolytes

Michael N. Kozicki and Maria Mitkova

Center for Solid State Electronics Research, Arizona State University, Tempe, Arizona 85287-6206, USA

ABSTRACT

Scalable elements that can be switched between widely-separated non-volatile resistance states at very low power are desirable for applications in next generation memory and logic. One potential approach involves the use of solid electrolyte films. A mobile metal ion-containing electrolyte film sandwiched between an oxidizable metal layer and an inert electrode constitutes a device which reversibly transitions between high and low resistance states. The resistance reduction occurs by the formation of a nanoscale conducting bridge created by reduction of the metal ions. A reverse bias dissolves the connection. Such polarity-dependent switching is attainable using voltages of a few hundred mV and currents in the μA range and can occur within a few tens of nanoseconds. In addition to possessing the endurance, retention, and CMOS compatibility required of future switching elements, such devices have excellent scaling prospects due to their low operational energy and demonstrated physical scalability. This paper reviews solid electrolyte resistance-change devices and discusses how the electrical characteristics of the most promising variants depend on the unique phase-separated nanostructure of the ion-containing films.

Key words: memory, resistance change, solid electrolyte, electrodeposition, nanostructure.

1. INTRODUCTION

It is widely accepted that the adoption of novel materials and radically different devices will be necessary to allow us to break through to the terabit regime in memory and processing[1]. One approach involves the use of material systems which lead to devices that can be switched between widely-separated non-volatile resistance states. Such elements could find widespread application in next generation memory, storage, and perhaps even logic. Whereas there are several technologies that show promise in this respect, they typically lack *complete* scalability, i.e., they have a physical size, programming voltage, or programming current that is excessive for high density integrated systems beyond the 32 nm node of the International Technology Roadmap for Semiconductors[2]. One potential approach to this issue involves the use of solid electrolyte films[3]. A mobile metal ion-containing electrolyte film sandwiched between an oxidizable metal layer (anode) and an inert electrode (cathode) constitutes a device which may be switched from a high to a low resistance state by the formation of a nanoscale conducting bridge created by reduction of the metal ions. A reverse bias dissolves the connection. Such polarity-dependent switching is attainable in the ten nanosecond regime and can be driven using voltages of a few hundred mV and currents in the μA range. In addition to possessing the endurance, retention, and CMOS compatibility required of future memory and storage elements, electrolyte-based devices have excellent scaling prospects due to their low operational energy and demonstrated physical scalability. Our own work in this area has focused mainly on devices with silver-doped germanium chalcogenide solid electrolyte films but we have also investigated copper as the mobile ion and electrolytes based on transition metal oxides[3,4]. This paper reviews solid electrolyte resistance-change devices and discusses how the electrical characteristics of the most promising variants depend on the unique nanostructure of the ion-containing films.

2. ELECTROCHEMICAL PRINCIPLES

The field of electrochemistry relates electrical phenomena to chemical changes in materials and vice-versa. An electron removed from an atom in the process of oxidation creates an ion and these charged species are able to move under the influence of an electric field in an electrolyte. Electrolytes can be solids as well as liquids. Indeed, some solids exhibit ion mobilities as high as those found in liquid electrolytes[5]. On receiving an electron, a displaced ion is reduced and becomes an atom. It is therefore possible to use the oxidation of a metal source, ion transport in an electrolyte, and reduction of ions to cause the *redistribution of mass*. The energy required to move the material is supplied by a power source via an external circuit.

An ion flow will only occur in an electrolyte if an oxidizable metal electrode is made positive with respect to an opposing electrode and sufficient bias, typically a few tenths of a volt or greater, is applied. The number of atoms electrodeposited by the reduction of ions will correspond to the number of electrons that take part in the process and these are supplied by the power supply in the external circuit. Each metal ion undergoing reduction will be balanced by a metal atom becoming oxidized and this avoids the formation of an internal electric field due to the build up of charge which would ultimately cancel the applied field and halt the electrodeposition. Note that if the opposite electrode is electrochemically inert (not oxidizable), the process is reversible by switching the polarity of the applied bias. When the electrodeposit is made positive with respect to the original oxidizable electrode, it becomes the new anode and will dissolve via oxidation. During the dissolution of the electrodeposit, the balance is maintained by deposition of metal back onto the place where the excess metal for the electrodeposition originally came from. Once the electrodeposit has been completely dissolved, the process self-terminates. It is important to note that it is the *asymmetry* of the device structure that allows the deposition/dissolution process to be cycled repeatedly.

The ability to move metallic mass via the application of a small voltage and current leads to a wide range of applications. We have previously demonstrated how this can be used to allow programmable interconnections in circuits[6], alteration of resonant frequency in microelectromechanical resonators[7], valving of fluid flow in microfluidic systems[8], and alteration of reflectance in optical elements[9]. However, it is the application of this technique in scalable resistance change elements that has attracted the most attention to date. In this case, the oxidation-transport-reduction process is used to form a nanoscale metallic filament within the electrolyte so that a low resistance path is created between the electrodes.

Many inorganic and organic (including polymeric) materials can conduct ions to some extent but it is the compounds of elements in the column of the Periodic Table headed by oxygen, the so-called *chalcogens*, that are of most interest in the context of electrochemical resistance-change devices, principally because of their high ion availability and mobility at normal device operating temperatures. We typically focus on those compounds that are best able to withstand the thermal processing used in integrated circuits at the back end of line (BEOL) – compounds of oxygen, sulfur, and selenium. Electrochemical switches have been fabricated using Cu_2S [10] and Ag_2S [11] binary chalcogenide electrolytes. The Cu_2S devices have been demonstrated in small memory arrays[12] and reconfigurable logic[13], and although the applications show promise, there is room for improvement in device performance factors such as retention and endurance with this particular electrolyte. The work on Ag_2S devices concentrated on switching by the deposition and removal of small numbers of silver atoms in a nanoscale gap between electrodes. This is of great significance as it demonstrates that the electrochemical switching technique has the potential to be scaled to single atom dimensions. Various oxide-based devices have also been demonstrated[14] and although these show great promise as easily integrated elements, the lower ion mobility in these materials tends to make the devices slower than in the case of the sulfide- and selenide-based electrolytes.

An alternative and intriguing approach is to create a highly stable solid electrolyte by combining S or Se with Ge to form a base glass into which we dissolve Cu or Ag. The combination can be achieved by diffusing the mobile metal from a thin surface film into a chalcogen-rich base glass (one which has more Se or S content than a stoichiometric composition) via *photodissolution*. The process utilizes light energy greater than the optical gap of the chalcogenide glass to create charged defects near the interface between the reacted and unreacted chalcogenide layers[15]. The holes created are trapped by the metal while the electrons move into the chalcogenide film. The electric field formed by the negatively charged chalcogen atoms and positively charged metal ions is sufficient to allow the ions to overcome the energy barrier at the interface and so the metal moves into the chalcogenide[16]. Prior to the introduction of the metal, the glass consists of GeS_4 ($GeSe_4$) tetrahedra and, in the case of the chalcogen-rich material, S (Se) chains. The introduced metal will readily react with the chain chalcogen and some of the tetrahedral material to form the ternary. This Ag-chalcogen reaction, which essentially nucleates on the chalcogen-rich regions within the base glass, results in a ternary that takes the form of a dispersed nanoscale metal-rich phase in a continuous glassy Ge-rich matrix[17,18]. We will discuss this unique nanostructure in more detail in the following section.

3. ELECTROLYTE NANOSTRUCTURE AND DEVICE PERFORMANCE

The composition and nanostructure of the solid electrolyte has a profound influence on its electrical and ionic characteristics so we will now consider this, using the Ag-Ge-Se ternary system as the example. If we assume that the Ag has a mean coordination of 3, the composition of ternary Ge-Se-Ag glasses may be represented as

$$(Ge_xSe_{1-x})_{1-y}Ag_y = (3y/2) (Ag_{2/3}Se_{2/3}) + (1-3y/2)(Ge_tSe_{1-t}) \tag{1}$$

where t is the amount of Ge in the Ge-Se backbone = $x(1-y)/(1-3y/2)$ [19]. For a Se-rich glass such as $Ge_{30}Se_{70}$, x = 0.30, and y = 0.333 at saturation, so we get t = 0.40. This means that the material consists of Ag_2Se and Ge_2Se_3 in the combination

$$16.7\ Ag_2Se + 10\ Ge_2Se_3 = Ag_{33}Ge_{20}Se_{47}. \qquad (2)$$

This electrolyte has a Ag_2Se molar fraction of 0.63 (16.7/26.7) and a Ag concentration of 33 at.% [20]. However, as mentioned previously, we have determined that the dissolution of Ag into a Se-rich base glass produces a ternary that is a combination of *separate* dispersed crystalline Ag_2Se and continuous glassy Ge-rich phases [21]. The spacing, s, between the Ag_2Se phase regions (and therefore the thickness of Ge_2Se_3 material between them) can be estimated by assuming that the crystalline regions are spherical and uniform in size and dispersion, so that

$$s = d(F_v^{-1/3} - 1) \qquad (3)$$

where d is the measured diameter of the crystalline Ag-rich phase and F_v is the volume fraction of this phase [22]. The volume fraction in the case of Ag_2Se in $Ag_{33}Ge_{20}Se_{47}$ is 0.57 (for a molar fraction of 0.63) so the average spacing between the Ag-rich regions is approximately 0.2 times their diameter. We determined the average diameter of the Ag_2Se crystallites using x-ray diffraction (XRD) techniques on blanket samples of Ag-diffused $Ge_{30}Se_{70}$ [22]. The average diameter of these regions was in the order of 7.5 nm, which means that by equation 3 above, they should be separated by approximately 1.5 nm of glassy Ge-rich material. This general structure has been confirmed by high resolution transmission electron microscopy (TEM). We have also performed XRD analysis on a sulfide-based ternary with similar stoichiometry, $Ag_{31}Ge_{21}S_{48}$, with much the same results. In this case, the Ag_2S crystallites were in the order of 6.0 nm in diameter [23]. We assume much the same nano-morphology exists in the case of Cu-doped films and are working to confirm this. It is important to note that the metal-rich phases are superionic mixed conductors (with resistivity as low a 2×10^{-3} Ω.cm in the case of Ag_2Se [24]) but the backbone material separating these conducting regions is a poor conductor so the overall resistivity of the electrolyte is high, typically well in excess of 100 Ω.cm. The distinctive nanostructure of this material leads to ideal characteristics in the context of switching devices as the high overall resistivity provides a high off resistance and the abundance of mobile ions is critical for rapid and stable resistance lowering.

When an oxidizable metal anode and an electrochemically inert cathode are formed in contact with a layer of a solid electrolyte, an applied voltage of a few hundred mV will reduce ions to form an electrodeposit of metal atoms $(Ag^+ + e^- \rightarrow Ag)$ and inject ions into the electrolyte via oxidation at the anode $(Ag \rightarrow Ag^+ + e^-)$. The Ag-rich regions within the ternary electrolyte will act as local ion supplies for the electrodepositon process and it is likely that growth will first occur in the high resistivity ($>10^6$ Ω.cm) glassy regions between them where the electric field is highest. This growth of the electrodeposit *within* the glassy solid is possible due to its void-rich, semi-flexible structure. The ions from the Ag-rich regions will be replaced via the ion current from the oxidizable electrode to preserve charge neutrality and electrons will be supplied from the negative electrode, mostly by way of the highly conducting growing electrodeposit. In the case of electrodeposition that is limited to a relatively small number of metallic bridges between crystallites, the overall resistance of the conducting pathway will be dominated by the resistivity of the superionic regions. An on resistance in the order of 20 kΩ in a 50 nm thick electrolyte would require a conducting region less than 10 nm in diameter for a Ag-Ge-Se electrolyte material. In the case where the electrodeposit dominates the pathway, i.e., the electrodeposted metal volume is greater than that of the superionic crystallites in the pathway, the electrodeposit resistivity (which is in the tens of μΩ.cm range) will determine the on resistance. In this case, a 10 nm diameter pathway will have a resistance in the order of 100 Ω. This means that the diameter of the conducting pathway will not exceed 10 nm for typical programming conditions which require on state resistances in the order of a few kΩ to a few tens of kΩ. The small size of the conducting pathway in comparison to the device area explains why on resistance has been observed to be independent of device diameter, whereas off resistance increases with decreasing area [25]. An electrodeposit this small means that the entire device can be shrunk to nanoscale dimensions without compromising its operating characteristics. This has been demonstrated by the fabrication of nanoscale devices as small as 20 nm that behave much like their larger counterparts [22,26]. The other benefit of forming a small volume electrodeposit is that it takes little charge to do so. The atomic density of Ag is 58 atoms/nm³ so, in an extreme case, if half the volume of a sub-10 nm diameter 50 nm long conducting region was pure Ag, only a few fC of Faradaic charge would be required to form a low resistance pathway.

The ions at the electron-supplying cathode will be reduced first and the site with the highest field and best ion supply will be favored for growth so that the electrodeposit extends out from the cathode, most likely at a single

location. Once the electrodeposit has grown from the cathode to the anode, the overall resistance of the device drops greatly. The decreasing resistance due to electrodeposition increases the current flowing through the device until the current limit of the source is reached. At this point, the voltage drop falls to the threshold for electrodeposition and the process stops, giving the final resistance value. Note that the electrodeposition threshold is actually lower than the initial "write" threshold as the voltage required to sustain electrodeposition is lower once an electrodeposit has started to form. To illustrate device operation, figures 1(a) and 1(b) give current-voltage and resistance-voltage plots respectively for a 240 nm diameter W/Ag-Ge-S/Ag device with a 60 nm thick electrolyte which has been annealed at 300 °C [4]. The voltage sweep runs from -1.0 V to +1.0 V to -1.0 V and the current limit is 10 µA. The write threshold depends on the electrode and electrolyte composition; for this material combination it is 450 mV (the threshold is 250 mV for W/Ag-Ge-Se/Ag devices). At this voltage, the device switches at from an off-state resistance, R_{off}, above 10^{11} Ω to an on-state resistance, $R_{on} = 22$ kΩ, more than six orders of magnitude lower for the 10 µA programming current. The apparent rise in resistance following switching is caused by the current limit control in the measurement instrument (an Agilent 4155C semiconductor parameter analyzer). Once electrodeposition is initiated, the threshold for further electrodeposition is decreased, as indicated by the presence of a lower voltage (220 mV) at which the current drops below the current limit on the negative-going sweep. R_{on} is determined by this voltage divided by the current limit (see below). The device transitions to a high resistance state at -250 mV and this is due to the initial breaking of the electrodeposited pathway by the reverse current flow. Continuing the negative sweep, the off resistance remains above 10^{11} Ω as the voltage is swept out to -1.0 V with a leakage current of less than 10 pA at maximum reverse bias.
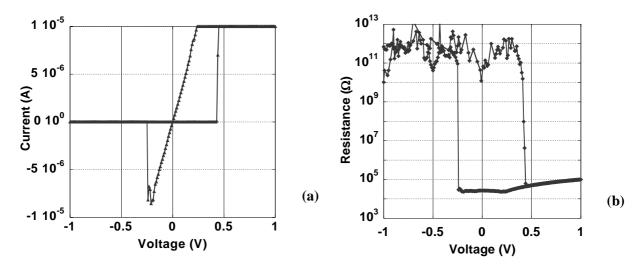

Figure 1. (a) Current–voltage plot of a 240 nm diameter device with a 60 nm thick Ag-Ge-S electrolyte using a 10 µA current limit. The device has been annealed at 300 °C. Voltage sweep is -1.0 V to +1.0 V to -1.0 V. (b) Resistance-voltage plot of the same device. Voltage sweep is -1.0 V to +1.0 V to -1.0 V (from ref. 4).

Figure 2 illustrates the dependence of R_{on} on the programming current limit, I_{prog}, in the range 1 to 10 µA for a W/Ag-Ge-Se/Ag device with a 50 nm thick electrolyte [3]. For this electrolyte/electrode combination, the write threshold is 240 mV and the electrodeposition threshold is 140 mV. R_{on} is related to I_{prog} by $R_{on} = 0.14/I_{prog}$ (the solid line in the figure). This relationship between electrodeposition voltage, programming current, and on resistance is common to all material combinations. It is explained by the fact that as long as sufficient potential difference is maintained for the situation where electrodeposition is already underway, in this case 140 mV, the reduction of silver ions will continue and the decrease in the resistance of the conducting bridge will be maintained even after it has formed. If the external current source is limited, once the resistance falls to a point where the voltage drop is no longer sufficient to support electrodeposition, the resistance lowering process ceases. The resulting resistance in ohms is therefore given approximately by the minimum potential to sustain electrodeposition in volts divided by the current limit of the external supply in amps.

The electrodeposit is electrically connected to the cathode and so it can supply electrons for subsequent ion reduction, effectively harvesting ions from the electrolyte, plating them onto its surface to extend itself forward. This means that the growing electrodeposit is always within a few nm of a source of ions in the electrolyte. For thin

electrolyte films, most of the applied voltage will be dropped across the polarized region where electrodeposition occurs. Since this is only a few tens of nm thick in these electrolytes, the field for an applied voltage of a few hundred mV will be in the order of 10^5 V/cm. Ion mobility at such fields can be in the order of 10^{-3} cm^2/V.s [5] and so the ions will join the growing electrodeposit at a velocity around 1 m/s, which also corresponds to the rate of the advancing growth front. Given this growth velocity, the intrinsic switching time of these devices will be 1 ns/nm of bridgeable path which is mostly the total length of the high resistivity regions in the electrolyte. Considering this, a device with an electrolyte around 50 nm thick will switch from its high resistance state to an electrodeposit-bridged low resistance state within a few tens of ns.
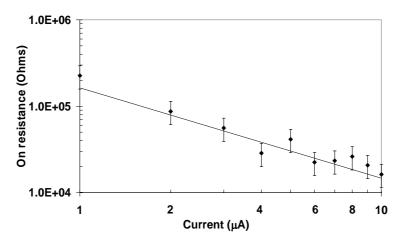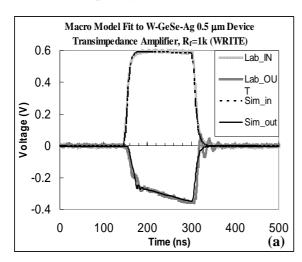

Figure 2. On-state resistance vs. programming current for a 1 μm diameter W/Ag-Ge-Se/Ag device. The resistance value in Ω is approximately 0.14 divided by the current in A (solid line), (from ref. 3).

The switching speed of a 500 nm diameter W/Ag-Ge-Se/Ag device with a 50 nm thick electrolyte is illustrated in figure 3, which shows both measured and simulated device results for write (figure 3(a)) and erase (figure 3(b)) operations[27]. For the write, a 150 ns pulse of 600 mV was applied to the device and the output of the transimpedance measurement amplifier shows that the device initially switches in less than 20 ns, ultimately reaching an on resistance of 1.7kΩ at the end of the write pulse. For the erase, a 150 ns pulse of -800 mV was applied and the output of the transimpedance measurement amplifier shows that the device transitions to a high resistance state (the start of the voltage decay in the output signal) in around 20 ns. This confirms the theoretical switching speed.
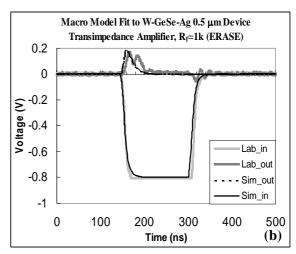

Figure 3. (a) Result of a 150 ns write pulse of 600 mV applied to a 500 nm W/Ag-Ge-Se/Ag device showing the output of the transimpedance measurement amplifier. The final on resistance is 1.7kΩ. (b) Result for a 150 ns erase pulse of -800 mV on the same device showing the output of the transimpedance measurement amplifier. Lab_in and Lab_out are the measured input and output signals and Sim_in and Sim_out are the corresponding model generated curves, (from ref. 27).

The electrodeposit is essentially metal that has been added to a chemically saturated electrolyte and this local supersaturation leads to high stability of the electrodeposit and excellent device retention characteristics. Figure 4 shows the results of a retention assessment test on a 2.5 μm diameter W/Ag-Ge-S/Ag device with a 60 nm thick electrolyte annealed at 300 °C, programmed using a 0 to +1.0 V sweep. The plot gives the off and on resistance measured using a 200 mV read voltage. The off state was in excess of 10^{11} Ω (above the limit of the measurement instrument) and remained undisturbed by the read voltage at this level for the duration of the test. The on resistance remained below 30 kΩ during the test. Following this test, the device was erased using a 0 to -1.0 sweep and the off state resistance measured using a 200 mV sensing voltage as before. The device remained above 10^{10} Ω beyond 10^5 s, demonstrating that the erased state was also stable. Other work has show that both on and off states are also stable at elevated temperature, with a margin of several orders of magnitude being maintained even after 10 years at 70 °C [26].

Note that if the electrodeposit is made positive with respect to the oxidizable electrode of the growth process, the electrodeposit itself is the anode and will dissolve via oxidation. During this dissolution, charge balance is maintained by electrodeposition of metal onto the oxidizable electrode. Once the electrodeposit has been completely dissolved, the erase process self-terminates. It is the asymmetry of the structure that allows cycling of the devices between a high resistance off state and a low resistance on state and thereby allows them to operate as high endurance memory elements. Figure 5 gives an example of cycling for a 75 nm Ag-Ge-Se electrolyte device[22]. Trains of positive (write) pulses of 1.2 V in magnitude and 1.6 μsec duration followed by -1.3 V negative (erase) pulses 8.7 μsec long were used to cycle the devices. These parameters were chosen to overcome the considerable parasitics of the test set-up. A 10 kΩ series resistor was used to limit current flow in the on state. The results are shown in 10^9 and 10^{11} cycle range. The data in figure 5 shows that there might be a slight decrease in on current but this is gradual enough to allow the devices to be taken well beyond 10^{11} write-erase cycles (if this decrease is maintained, there will only be a 20% decrease in on current at 10^{16} cycles).
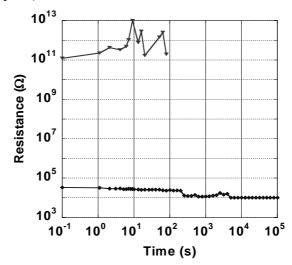

Figure 4. Off- (upper plot) and on-state (lower plot) resistance vs. time measured using a 200 mV read voltage for a 2.5 μm W/Ag-Ge-S/Ag device programmed using a 10 μA current limit. Off-state resistance remained above 10^{11} Ω for the duration of the test.

4. CONCLUSIONS

This paper has reviewed resistance change devices based on solid electrolytes. The nano-heterogeneous (nano phase-separated) nature of ternary electrolytes leads to excellent device characteristics, including high off resistance and a fast transition to a stable low resistance on state. A reduction in resistance of several orders of magnitude is attainable for a write power as low as 250 nW (1 μA program current in Ag-Ge-Se devices). The on resistance is a function of write current, which makes multi-level cell operation with simple sensing schemes a possibility, and extrapolated retention results suggest that the reduced resistance (with a large off to on ratio) will persist for over 10 years. Simulated and measured results show that the devices write and erase within 20 ns and further scaling, especially in the vertical dimension, is likely to result in even greater programming speeds. Note that write times in the order of a few tens of nsec mean that the write energy is less than 100 fJ, which makes PMC one of the lowest energy non-volatile memories. Even sub-100 nm devices show excellent endurance with no significant degradation to over 10^{10}

cycles with stable operation indicated well beyond this. The low resistivity and small size of the electrodeposits mean that the entire device can be shrunk to nanoscale dimensions without compromising operating characteristics. The physical scalability, combined with low voltage and current operation, suggests that extremely high storage densities will be possible. The other benefit of forming a small volume electrodeposit is that it takes little charge to do so – in the order of a few fC to create an extremely stable low resistance link. The charge required to switch a PMC element to a non-volatile state is therefore comparable to the charge required for *each* refresh cycle in a typical DRAM.
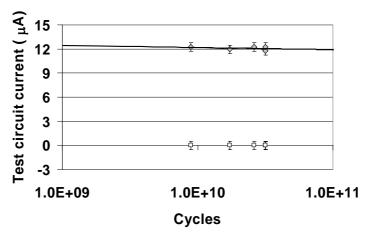

Figure 5. Current in the on (upper plot) and off (lower plot) state at various numbers of cycles for a 75 nm Ag-Ge-Se device. The device was cycled using trains of positive (write) pulses of 1.2 V in magnitude and 1.6 µsec duration followed by -1.3 V negative (erase) pulses 8.7 µsec long. The solid line is a logarithmic fit to the on current data (from ref. 22).

REFERENCES

1. G. Müller, T. Happ, M. Kund, G.Y. Lee, N. Nagel, and R. Sezi, "Status and outlook of emerging nonvolatile memory technologies," IEDM Tech. Dig., 567-570, (2004).

2. The International Technology Roadmap for Semiconductors may be obtained from http://public.itrs.net.

3. M.N. Kozicki, C. Gopalan, M. Balakrishnan, M. Park, and M. Mitkova, "Non-volatile memory based on solid electrolytes," Proceedings of the 2004 Non-Volatile Memory Technology Symposium, 10-17, Orlando, Florida, November, 2004.

4. M.N. Kozicki, M. Balakrishnan, C. Gopalan, C. Ratnakumar, and M. Mitkova, "Programmable Metallization Cell memory based on Ag-Ge-S and Cu-Ge-S solid electrolytes," IEEE Non-Volatile Memory Technology Symposium, D5, 1-7 (2005).

5. T. Kawaguchi, S. Maruno, and S.R. Elliott, "Optical, electrical, and structural properties of amorphous Ag–Ge–S and Ag–Ge–Se films and comparison of photoinduced and thermally induced phenomena of both systems," J. Appl. Phys., vol. 79, 9096-9104 (1996).

6. M.N. Kozicki, M. Yun, L. Hilt, and A. Singh, "Applications of programmable resistance changes in metal-doped chalcogenides", Proceedings of the 1999 Symposium on Solid State Ionic Devices, Editors - E.D. Wachsman et al., The Electrochemical Society, Inc., 1 - 12 (1999).

7. S. Enderling, C. L. Brown III, M. Balakrishnan, J. Hedley,J.T.M. Stevenson, S. Bond, C.C. Dunare, A.J. Harris, J.S. Burdess, M. Mitkova, M.N. Kozicki, and A.J. Walton, "Integration of a novel electrochemical tuning scheme with MEMS surface micromachined resonators", IEEE MEMS 05, Miami, Florida, January 2005.

8. M.N. Kozicki, P. Maroufkhani, M. Mitkova, "Flow regulation in microchannels via electrical alteration of surface properties", Superlattices and Microstructures, Vol 34, 467 (2004).

9. J. P. Aberouette, "Optical applications of Programmable Metallization Cell", Masters Thesis, Arizona State University, 2002.

10. T. Sakamoto, H. Sunamura, H. Kawaura, T. Hasegawa, T. Nakayama, and M. Aono., "Nanometer-scale switches using. copper sulfide," Appl. Phys. Lett., vol. 82, 3032 (2003).

11. K. Terabe, T. Hasegawa, T. Nakayama, M. Aono, "Quantized conductance atomic switch" Nature, vol. 433, 47 (2005).

12. S. Kaeriyama, T. Sakamoto, H. Sunamura, M. Mizuno, H. Kawaura, T. Hasegawa, K. Terabe, T. Nakayama, and M. Aono, "A nonvolatile programmable solid-electrolyte nanometer switch," IEEE J. Sol. St. Ccts., vol. 40, 168 (2005).

13. T. Sakamoto, N. Banno, N. Iguchi, H. Kawaura, S. Kaeriyama, M. Mizuno, K. Terabe, T. Hasegawa, M. Aono, IEDM Tech. Dig. 19.5, 2005.

14. M.N. Kozicki, C. Gopalan, M. Balakrishnan, and M. Mitkova, "A Low Power Non-Volatile Switching Element Based on Copper-Tungsten Oxide Solid Electrolyte," IEEE Trans. Nanotechnology, in press.

15. J. H. S. Rennie, S. R. Elliott, "Investigations of the Mechanism of Photo-dissolution of Silver in Amorphous Germanium chalcogenide Thin Films," J. Non-Cryst. Sol., vols. 97/98, 1239 (1987).

16. A. V. Kolobov, S. R. Elliott, M. A. Taguirdzhanov, "On the Mechanism of Photodoping in Vitreous Chalcogenides", Phil. Mag. *B* 61, 857 (1990).

17. M. Mitkova, M. N. Kozicki, H. Kim, T. Alford, "Local Structure Resulting From Photo- and Thermal Diffusion of Ag in Ge-Se Thin Films," J. Non-Cryst. Sol., vol. 338-340C, 552-556 (2004).

18. M. Mitkova, M.N. Kozicki, H.C. Kim, and T.L. Alford, "Thermal and Photodiffusion of Ag in S-Rich Ge-S amorphous films," Thin Solid Films, vol. 449, 248-253 (2004).

19. M. Mitkova, Y. Wang, P. Boolchand, "The Dual Chemical Role of Silver as Dopant in the Ge-Se-Ag Ternary," Phys. Rev. Lett., vol. 83, 3848 (1999).

20. M. Mitkova and M.N. Kozicki, "Silver Incorporation in Ge-Se Glasses Used in Programmable Metallization Cell Devices," J. Non-Cryst. Solids, vol. 299-302, 1023 (2002).

21. M.N. Kozicki, M. Mitkova, J. Zhu, and M. Park, "Nanoscale phase separation in Ag-Ge-Se glasses," Microelectronic Engineering, vol. 63, 155-159 (2002).

22. M.N. Kozicki, M. Park, and M. Mitkova, "Nanoscale memory elements based on solid state electrolytes," IEEE Trans. Nanotechnology, vol. 4, no. 3, 331-338 (2005).

23. M. Balakrishnan, M.N. Kozicki, C.D. Poweleit, S. Bhagat, T. L. Alford, and M.Mitkova, "Crystallization effects in annealed thin GeS_2 films photodiffused with Ag," J. Non-Cryst. Sol., in press.

24. S. Miyatani, "Electrical properties of pseudo-binary systems of Ag_2VI's; $Ag_2Te_xSe_{1-x}$, $Ag_2Te_xS_{1-x}$, and $Ag_2Se_xS_{1-x}$," J. Phys. Soc. Japan, vol. 15, 1586 (1960).

25. R. Symanczyk, M. Balakrishnan, C. Gopalan, U. Grüning, T. Happ, M. Kozicki, M. Kund, T. Mikolajick, M. Mitkova, M. Park, C. Pinnow, J. Robertson, and K. Ufert, "Electrical characterization of solid state ionic memory elements," Proceedings of the 2003 Non-Volatile Memory Technology Symposium, 17-1, San Diego, California, November 2003.

26. M. Kund, G.Beitel, C. Pinnow, T. Röhr, J. Schumann, R. Symanczyk, K. Ufert, and G. Müller, "Conductive Bridging RAM (CBRAM): An emerging non-volatile memory technology scalable to sub 20nm", IEDM Tech. Dig., 31.5, 2005.

27. Nad E. Gilbert, Chakravarthy Gopalan, and Michael N. Kozicki, "A macro model of programmable metallization cell devices," Solid State Electronics, vol. 49, 1813–1819 (2005).